0026-895X/96/051200-07$3.00/0
Copyright © by The American Society for Pharmacology and Experimental Therapeutics
All rights of reproduction in any form reserved.
MOLECULAR PHARMACOLOGY, 50:1200–1206 (1996).

Novel Antagonists of the Inhibitory Glycine Receptor Derived from Quinolinic Acid Compounds

VOLKER SCHMIEDEN, SYLVIE JEZEQUEL, and HEINRICH BETZ

Department of Neurochemistry, Max-Planck-Institute for Brain Research, D-60528 Frankfurt/Main, Germany

Received May 28, 1996; Accepted July 15, 1996

SUMMARY

Binding of the coagonist glycine to the *N*-methyl-D-aspartate (NMDA) subtype of glutamate receptors is potently antagonized by 2-carboxy-4-hydroxyquinolines. We show that closely related derivatives, 4-hydroxy-quinolines and 4-hydroxquinoline-3-carboxylic acids, antagonize the agonist response of the recombinant inhibitory glycine receptor (GlyR). In *Xenopus laevis* oocytes expressing the GlyR α1 subunit, the chloride-substituted derivatives 5,7-dichloro-4-hydroxyquinoline-3-carboxylic acid and 7-chloro-4-hydroxyquinoline inhibited glycine currents in a mixed high affinity competitive and low-affinity noncompetitive fashion, whereas the related compounds 7-trifluoromethyl-4-hydroxyquinoline-3-carboxylic acid and 7-trifluoromethyl-4-hydroxyquinoline showed purely competitive antagonism. Our data suggest a model of the pharmacophore of the GlyR that displays significant similarity to that proposed for the glycine binding site of the *N*-methyl-D-aspartate receptor.

The inhibitory GlyR is a ligand-gated anion channel protein that mediates postsynaptic inhibition in spinal cord, brainstem, and other regions of the central nervous system (1). It consists of homologous ligand-binding α (α1-4) (2–5) and structural β (6) subunits, which share an extended amino-terminal extracellular domain and four membrane-spanning segments each. In the native hetero-oligomeric GlyR, α and β subunits are assembled at a 3:2 stoichiometry (7). However, expression of single α subunits in *Xenopus laevis* oocytes (4, 8, 9) or mammalian cells (10) generates homo-oligomeric glycine-gated channels, whose pharmacology closely resembles that of the native GlyR. Thus, the major determinants of agonist and antagonist binding seem to be localized on the α subunits.

Although the GlyR constitutes a key regulator of both motor and sensory pathways (11, 12), little is known about its pharmacophore. In addition to the classic GlyR antagonist strychnine, different unrelated compounds have been described, all of which inhibit glycine responses (13). Most of these, however, are also active at the γ-aminobutyric acid type A receptor (13) and therefore do not represent GlyR-selective agents. The repertoire of GlyR agonists is rather small; other than glycine, the amino acids β-alanine and taurine are the only potent activators of ion flux. Mutational analysis has been used to identify distinct amino acid side chains required for agonist and antagonist binding (9, 14–21); a precise picture of the ligand binding pocket of the GlyR, however, is only beginning to emerge from these studies.

The excitatory NMDAR requires glycine as a coagonist in addition to glutamate for efficient gating (22). The pharmacology of its glycine binding site, however, is rather distinct from that of the GlyR (23). Different glycine site agonists of the NMDAR have been derived from the α-amino acid structure; these ligands display a marked stereoselectivity for binding in their respective D-configuration (23). The agonist binding site of the GlyR, in contrast, shows a high preference for L-amino acids (24). Potent glycine antagonists of the NMDAR have been prepared using 2-carboxy-4-hydroxyquinoline as a lead compound. The affinities of these ligands are increased on lipophilic substitution, as found in 5,7-dichlorokynurenic acid (25).

In this study, we show that hydroxyquinoline derivatives, which contain a carboxylic acid substitution at the third ring atom, potently inhibit the glycine response of the recombinant α1 subunit GlyR. Importantly, these compounds are GlyR selective and inactive at the NMDAR and therefore define a novel class of GlyR antagonists.

Materials and Methods

The methods used for analysis of the pharmacology of recombinant GlyR and NMDAR have been described previously (8, 26, 27). Briefly, *X. laevis* oocytes were removed from frogs that had been

This work was supported by Fonds der Chemischen Industrie and the Human Capital and Mobility Program (ERBCHRXCT 930167).

ABBREVIATIONS: GlyR, glycine receptor; Q3A, quinoline-3-carboxylic acid; Q4A, quinoline-4-carboxylic acid; 6ClQA, 6-chloro-4-hydroxyquinoline-3-carboxylic acid; 7TFQ, 7-trifluoromethyl-4-hydroxyquinoline; 7TFQA, 7-trifluoromethyl-4-hydroxyquinoline-3-carboxylic acid; 7ClQA, 7-chloro-4-hydroxyquinoline-3-carboxylic acid; 5,7ClQA, 5,7-chloro-4-hydroxyquinoline-3-carboxylic acid; NMDAR, *N*-methyl-D-aspartate receptor; DMSO, dimethylsulfoxide.

anesthetized with urethane (Sigma Chemical, Munich, Germany), dissected after collagenase (Sigma) treatment, and injected with cRNAs of the human GlyR α1 subunit (10–20 ng/oocyte) or the NMDAR subunits NR1 from rat and NR2B from mouse (10–20 ng each), synthesized through *in vitro* transcription (mCAP kit; InVitrogen, Leek, The Netherlands) as described previously (8, 27). Voltage-clamp recording of whole-cell currents was performed 24–48 hr after injection at a holding potential of −70 mV. Experimental values are presented as the mean ± standard error of peak current responses. For the evaluation of half-maximal effective agonist concentrations (EC_{50}) and Hill coefficients (h) from dose-response curves, data from several oocytes were fitted using the least-squares equation (26). Inhibition curves were obtained by coapplication of glycine at a concentration corresponding to its EC_{50} value with increasing concentrations of antagonist. Wash-out times between each application were 3–5 min.

All drugs used in the present study were purchased from Aldrich (Steinheim, Germany), with the exception of 5,7-dichloro-4-hydroxyquinoline-3-carboxylic acid, which was synthesized by Hartmut Guchhalla (University of Mainz, Mainz, Germany). Quinoline carboxylic acids and quinolinols (Fig. 1) were dissolved in DMSO to prepare 10 or 50 mM stock solutions, respectively, and freshly diluted with frog Ringer's solution to the desired final concentrations.

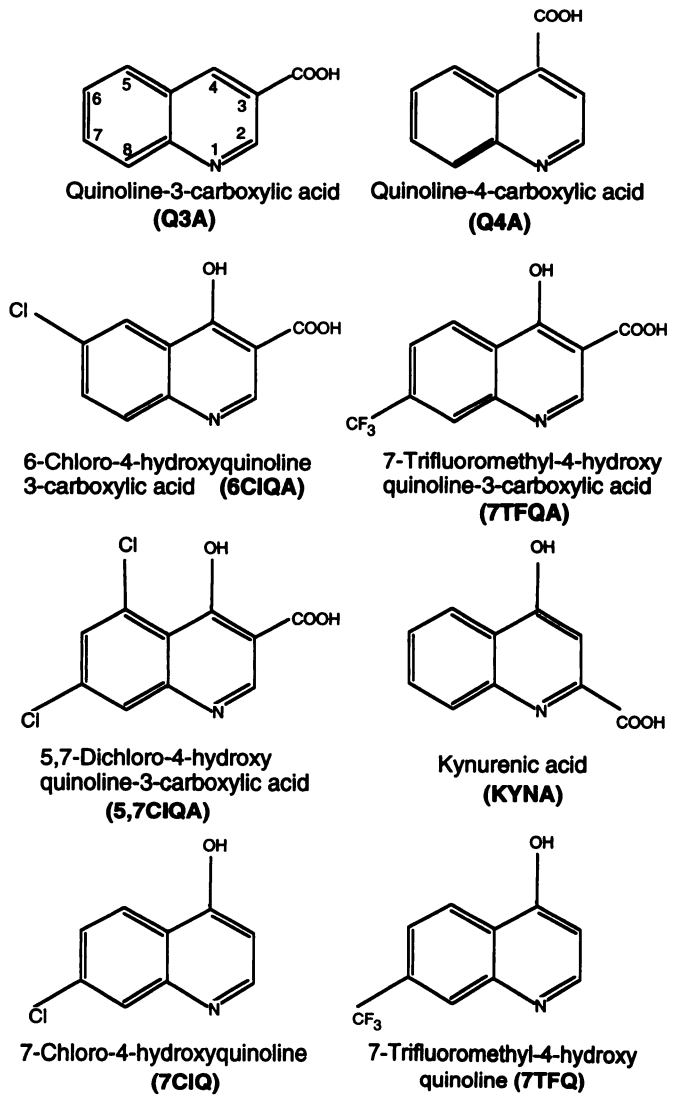

Fig. 1. Structures of the quinolinic acid and quinolinole derivatives used in the study. *Parentheses*, abbreviations.

Results

Quinoline carboxylic acid compounds. As reported previously (26), heterocyclic piperidine analogs exhibit antagonist activities at the GlyR, when acidic and hydroxyl group substitutions are positioned at the C3 and C4 ring carbon atom, respectively. In contrast, piperidine analogs with substitutions at the C2 atom are inactive. We therefore analyzed the effects of Q3A and Q4A, respectively, on GlyR function. Both derivatives elicited no current response on superfusion up to a concentration of 100 μM (Fig. 2A). In the presence of 180 μM glycine [i.e., a concentration that produced a half-maximal response (EC_{50})], each compound reduced the agonist-evoked current by only 10–20% (Fig. 2A). Higher concentrations of these ligands could not be used because solutions containing >1% of the solvent DMSO produced an inhibition of glycine responses (data not shown). Nevertheless, Fig. 2A demonstrates that Q4A was slightly more potent in GlyR antagonism than Q3A.

Hydroxylated and halogen-substituted quinolinic acids. Hydroxylated and halogen-substituted analogs of the above-mentioned quinoline carboxylic acids behaved as more potent antagonists at the GlyR. The current response produced by 180 μM glycine was reduced by 46 ± 4.6% (seven oocytes) in the presence of 100 μM 6ClQA and by 82 ± 5% (five oocytes) in the presence of 100 μM 7TFQA. To examine whether multiple chloride substitutions at ring positions 5 and 7 of the quinolinic acid compounds increase high affinity binding to the GlyR, as is known to occur for the NMDAR, in which 5,7-dichlorokynurenic acid is a potent antagonist (25),

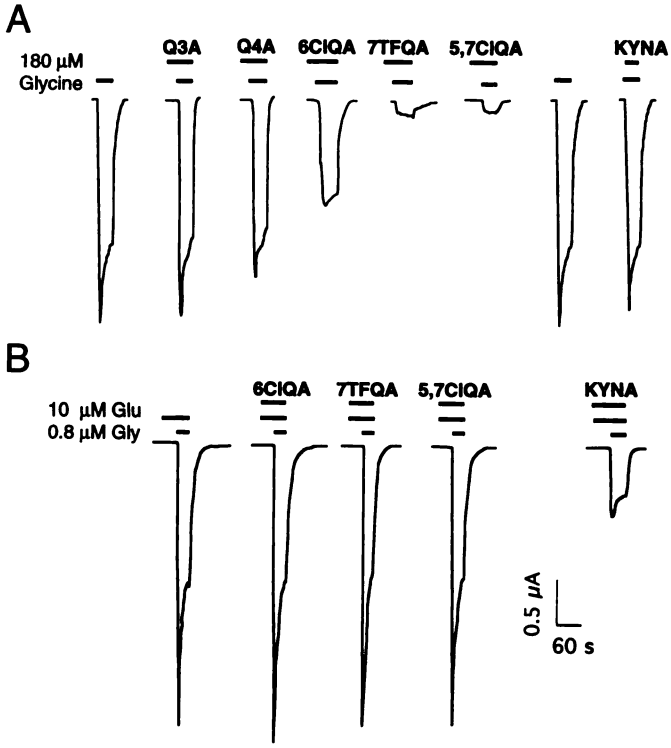

Fig. 2. Inhibition of glycine (*Gly*)-induced currents by quinolinic acids in α1 GlyR (A) and NMDAR (B) -expressing oocytes. *Bars above traces*, duration of drug application. Note that preapplication of quinolinic acids without glycine (A) or with glutamate (*Glu*) (B) failed to produce current responses. All compounds were applied at a concentration of 100 μM.

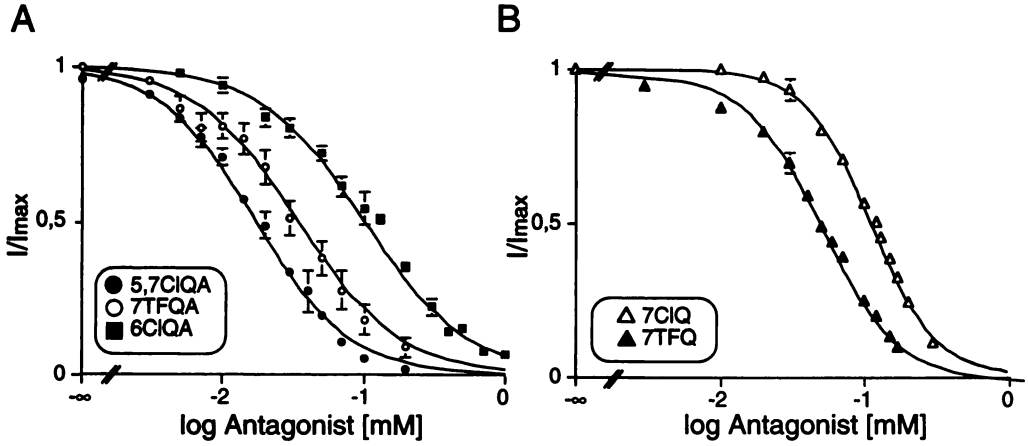

Fig. 3. GlyR antagonism by quinoline derivatives. Glycine (230 μM) was coapplied with increasing concentrations of the indicated quinolinic acid (A) and quinolinol (B) compounds. Current values were normalized to the glycine response obtained in the absence of antagonist and fitted by a single sigmoidal curve (mean ± standard error from three to seven oocytes). *Error bars* often were smaller than the symbols used and so were not indicated.

5,7ClQA was also tested. Fig. 2A shows that a 100 μM concentration of the latter compound inhibited the glycine-evoked current by 95 ± 10% (five oocytes). In contrast, at the NMDAR, 6ClQA, 7TFQA, and 5,7ClQA (all 100 μM) had no effect on the current response evoked by coapplication of glutamate (10 μM) and glycine (0.8 μM) (Fig. 2B). Kynurenic acid (4-hydroxyquinoline-2-carboxylic acid), however, inhibited the glycine response of the NMDAR but not that of the GlyR (Fig. 2).

Fig. 3A shows concentration-effect curves of GlyR inhibition for all three quinolinic acid derivatives, which indicate IC_{50} (concentration required for half-maximal inhibition) values of 19.4 ± 5.1, 36.1 ± 5.8, and 118.5 ± 11.8 μM for 5,7ClQA, 7TFQA, and 6ClQA, respectively, and Hill coefficients of ≥1.4 for all compounds (Table 1). Thus, halogen substitutions at positions 5 and 7 of the quinolinic acid structure seem to be important for efficient GlyR antagonism. In addition, the affinity of quinolinic acid derivatives is increased by carboxyl and hydroxyl substitutions at positions 3 and 4, respectively. The noncarboxylated quinolinols 7TFQ and 7ClQ exhibited IC_{50} values ~2-3-fold higher than their acidic analogs (Fig. 3B and Table 1).

Analysis of GlyR antagonism. To evaluate the mechanism of GlyR inhibition by the aforementioned quinoline derivatives, we determined the concentration-effect curves of glycine in the absence and presence of the different antagonists.

5,7ClQA, applied at a concentration corresponding to its IC_{50} value (20 μM), shifted the concentration-response curve of glycine to higher concentrations without altering its slope or maximal amplitude (Fig. 4A); this behavior is typical for a competitive antagonist. At higher antagonist concentrations (50 μM), however, the maximally evoked glycine response decreased by ≤20%, which indicates additional noncompetitive inhibition (Fig. 4A). Both competitive and noncompetitive inhibition was also seen at holding potentials of −50 and −90 mV (data not shown); this argues against a channel block by this compound. Similar results were obtained with 7ClQ, which produced a significant reduction of the maximal glycine response at high concentrations (Fig. 4B). We therefore classify 5,7ClQA and 7ClQ as mixed competitive/noncompetitive antagonists. In contrast, 7TFQA and 7TFQ seemed to be purely competitive inhibitors because a full recovery of maximal glycine currents could be obtained even in the presence of 100 and 200 μM concentrations, respectively, which is 3–4-fold higher than the respective IC_{50} values of these compounds (Fig. 4, C and D, and below).

TABLE 1

GlyR pharmacology of quinoline derivatives

Inhibition of glycine currents by quinoline derivatives was analyzed in oocytes injected with GlyR α1 cRNA. IC_{50} values and Hill coefficients (*h*) are from experiments using glycine at a half-saturating concentration of 230 μM.

Antagonist	IC_{50}	*h*	No. of oocytes	K_i[a]
	μM			μM
5,7ClQA	19.4 ± 5.13	1.44 ± 0.13	5	30
7TFQA	36.1 ± 5.77	1.65 ± 0.07	10	48
7TFQ	51.2 ± 2.39	1.72 ± 0.05	3	115
7ClQ	115.0 ± 3.30	1.87 ± 0.03	4	300
6ClQA	118.5 ± 11.8	1.33 ± 0.21	7	N.D.[b]

[a] For the calculation of K_i values, see the text.
[b] Not determined because of low affinity inhibition.

To more precisely examine the noncompetitive interaction of 5,7ClQA and 7ClQ and to exclude a possible modulation of ligand binding by DMSO, we coapplied increasing concentrations of these antagonists with 0.14, 0.2, 0.3, 0.5, 0.7, and 1 mM glycine, respectively. The resulting inhibition curves for 5,7ClQA (Fig. 5A) and 7ClQ (data not shown) had the same slope and were simply shifted to the right, even in the presence of high concentrations of glycine. The respective IC_{50} values increased 5–6-fold from 11 ± 4 to 63 ± 19 μM and from 105 ± 5 to 570 ± 70 μM, respectively, whereas the Hill coefficients remained unchanged (1.5–1.8; see Fig. 5A). In contrast, the slopes of the dose-response curves for the fluoromethyl-substituted analogs, 7TFQ and 7TFQA, increased significantly when the glycine concentration was increased, as revealed by a respective change in Hill coefficient from 1.5 to 2.3 (Fig. 5B and data not shown). Simultaneously, the IC_{50} values increased almost 10-fold, from 15 to 120 μM and from 55 to 500 μM, respectively. This corroborates that the mechanism of antagonism by chloro- and trifluoromethyl-substituted quinoline compounds is different and unaffected by the solvent.

When plotting the measured IC_{50} values against glycine concentration, nonlinear correlations emerged (Fig. 5, C–F). Because the data could not be fitted by a simple Cheng-Prusoff equation, we used the procedure proposed by Leff and Dougall (28) for analysis of the binding of cooperative ligands:

$$IC_{50} = K_i\left(\sqrt[h]{2+\left(\frac{A}{EC_{50}}\right)^h} - 1\right)$$

This equation describes a hyperbolic curve, in which *h* is the Hill coefficient, EC_{50} is the half-maximal response of the

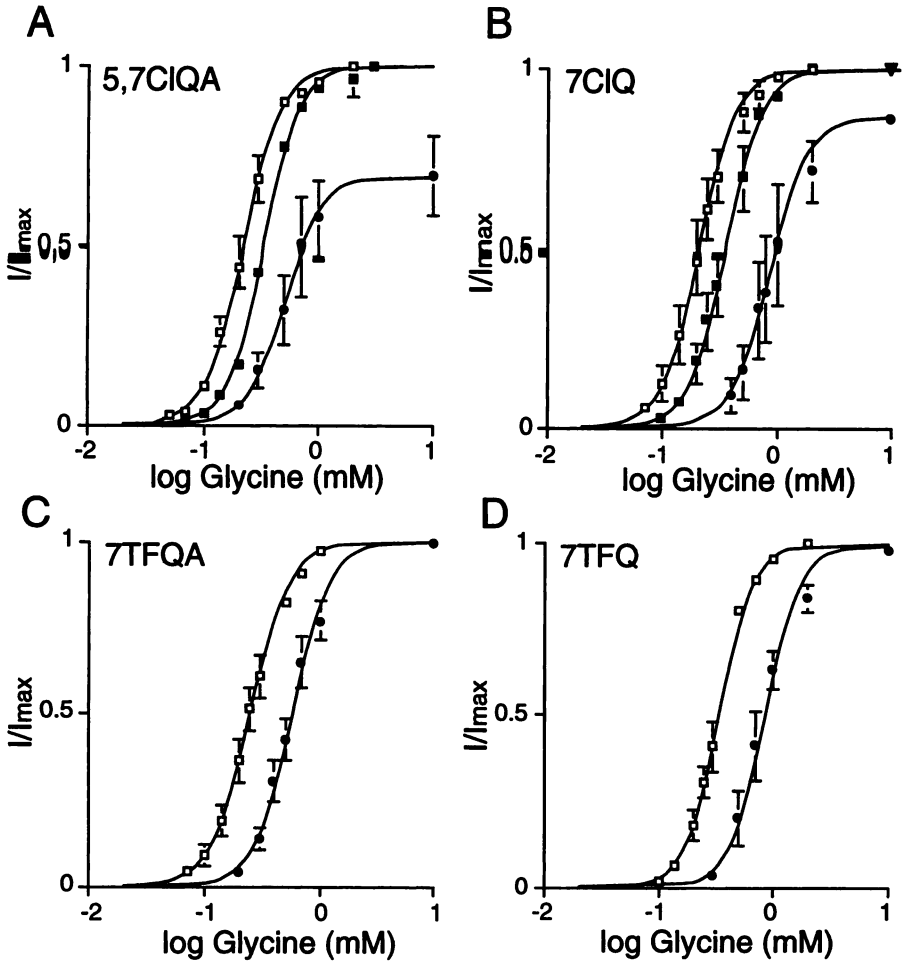

Fig. 4. Competitive inhibition of glycine responses by quinoline derivatives. A, Glycine dose-response curve in the absence (□) and presence of 5,7ClQA at concentrations of 20 μM (■) and 50 μM (●). B, Same experiment as A but in the presence of 7ClQ at concentrations of 100 μM (■) and 500 μM (●). C, Same experiment as A but in the presence of 100 μM 7TFQA (●). D, Same experiment as A but in the presence of 200 μM 7TFQ (●). Note the differences in residual I_{max} values between A and B and between C and D when antagonists were used at concentrations that were 3–5-fold higher than their respective IC_{50} values.

agonist (A), and K_i is the inhibition constant of the antagonist. By using the experimentally determined values, the data were analyzed and fitted to the predicted IC_{50} values of a fully competitive antagonist (28). Using an EC_{50} value of 230 μM and a Hill coefficient of 2.6 deduced from the glycine dose-response curve, a fully competitive behavior of 7TFQA and 7TFQ was confirmed, as indicated by a perfect fit of the experimental and calculated IC_{50} values (Fig. 5, D–F). However, the chloride-substituted quinolines exhibited a mixed behavior, with competitive inhibition at low concentrations of glycine and noncompetitive inhibition at high concentrations of glycine (Fig. 5, C–E). These results corroborate the conclusions given above. Interestingly, the K_i values of all antagonists calculated according to Eq. 1 were higher than the experimentally determined IC_{50} values (Table 1). This contrasts with traditional Cheng-Prusoff calculations, which result in K_i values that are lower than the measured IC_{50} value. Consequently, the use of Cheng-Prusoff equations will lead to an overestimation of antagonist affinity, a conclusion already reached in the theoretical considerations of Leff and Dougall (28).

Discussion

In the current study, we analyzed the effects of several quinolinic acid derivatives on GlyR function and found a strong inhibition of the glycine response by compounds containing a carboxylic group at the third carbon atom of the heterocyclic ring system. Furthermore, both purely competitive and competitive/noncompetitive antagonisms were observed on substitution of the aromatic ring by a trifluoromethyl or a chloride group, respectively.

Although both the GlyR and the NMDAR bind glycine as a principal agonist, the pharmacology of their glycine binding sites is very distinct. Notably, many heterocyclic compounds containing a nitrogen atom and the carboxylic group in a configuration that mimics glycine are active at the NMDAR but inactive at the GlyR. As demonstrated previously by the analysis of α-amino acids and piperidine carboxylic acid analogs, small uncharged groups near the nitrogen atom seem to be important for efficient GlyR binding (26). In addition, a defined distance between the carboxylic group and the nitrogen is crucial for antagonist activity, as revealed by the potencies of different piperidine 3-carboxylic acid derivatives and β-amino acids (26). The latter molecules are partial agonists that display both agonistic and antagonistic behavior, with EC_{50} values being consistently higher than their respective IC_{50} values. To account for these different activities, a binding model has been proposed for the GlyR in which the activity of β-amino acids is determined by their molecular conformation, with *cis*-conformers displaying agonistic and *trans*-conformers displaying antagonistic potencies (26). A β-amino acid *trans*-configuration is also found in nipecotic acid and guavacine, both of which antagonize the GlyR response (26). In addition, potent inhibition of glycine-evoked currents was seen with isonipecotic acid and isoguavacine, both of which contain a folded γ-aminobutyric acid motif (26).

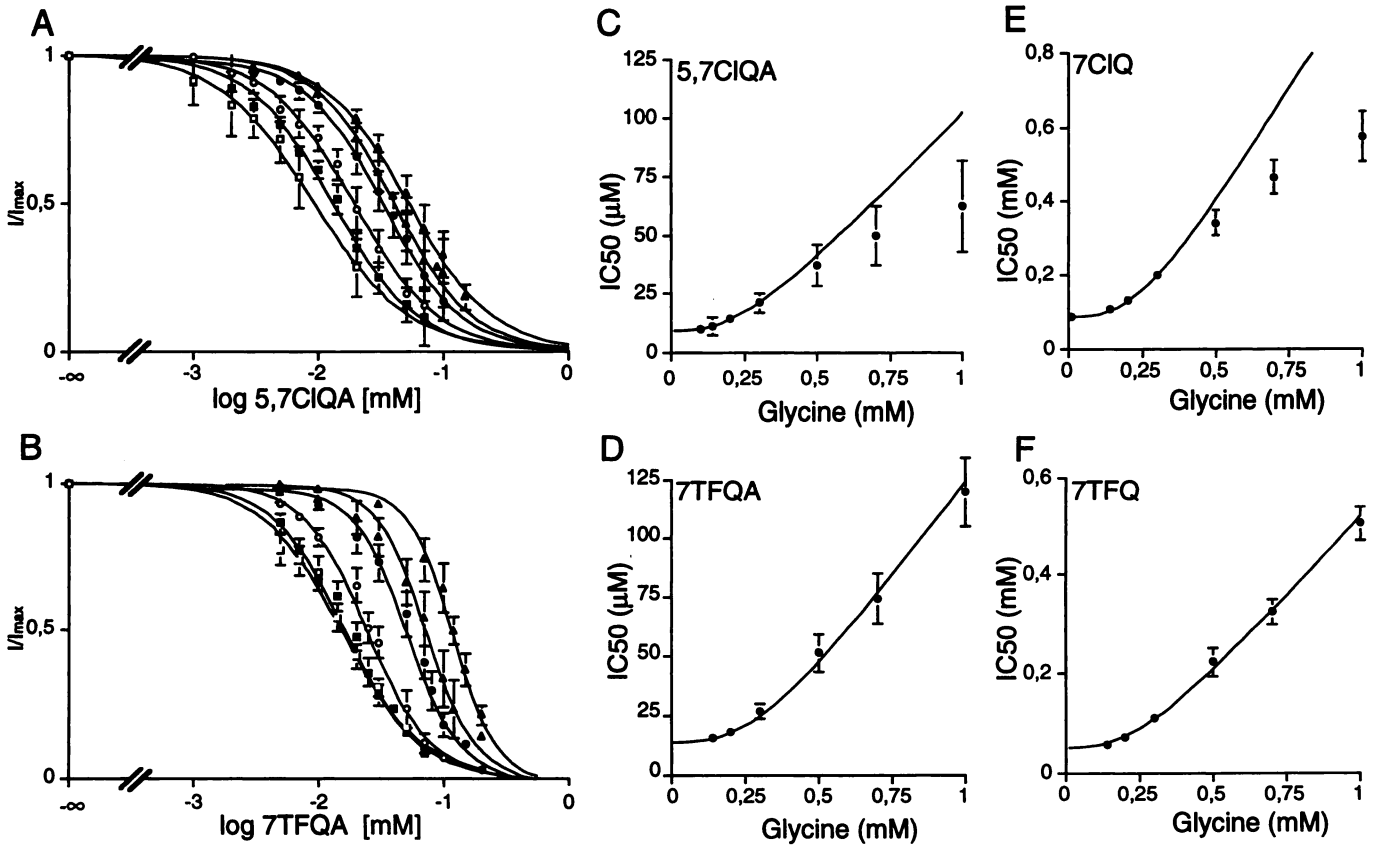

Fig. 5. Analysis of GlyR current inhibition by quinoline derivatives. Glycine at concentrations of 140 μM (□), 200 μM (■) 300 μM (○), 500 μM (●), 700 μM (△), and 1 mM (▲) was coapplied with increasing concentrations of 5,7ClQA (A) or 7TFQA (B). The IC_{50} values obtained from individual inhibition curves shown in A and B were plotted against glycine concentration for 5,7ClQA (C), 7TFQA (D), 7ClQ (E), and 7TFQ (F). *Data points*, fit as described in the text. Note that 5,7ClQA (C) and 7ClQ (E) show a competitive inhibition behavior at low concentrations of glycine; at higher concentrations, inhibition becomes noncompetitive, as revealed by a deviation of the data points from the exponential fit. 7TFQA (D) and 7TFQ (F), in contrast, behaved as fully competitive antagonists, even at high agonist concentration.

Here, we extended our analysis of carboxyl group positioning in GlyR active compounds by testing several 4-hydroxyquinoline-3-carboxylic acid derivatives. All compounds containing an acidic residue at the third position of the heterocyclic ring and a hydroxylic group at the fourth position behaved as GlyR antagonists. In contrast, 4-hydroxyquinoline-2-carboxylic acids such as kynurenic acid (Ref. 29 and this study) and 5,7-dichloro-kynurenic acid (29) displayed no activity; this underlines the crucial role of the β-amino acid *trans*-configuration for antagonistic binding to the GlyR. However, Q3A and Q4A, which carry only a carboxyl group, were rather poor antagonists. Thus, a hydroxyl group at position 4 of the aromatic heterocycle is important for high affinity binding. Also, the potency of the quinolinole 7TFQ was lower than that of its acidic analog, 7TFQA, indicating that the carboxyl and hydroxyl groups of the heterocycle constitute synergistic determinants of antagonist binding.

Of all quinolinic acid compounds tested, 5,7ClQA (containing two chloride substituents) was the most potent antagonist. Apparently, lipophilic substituents at positions 5 and 7 are major determinants of high affinity binding, whereas a single chloride substitution at position 6 is less effective. Trifluoromethyl side chains also generated potent antagonists. Because the IC_{50} value of 7TFQ was 2-fold lower than that of 7ClQ, trifluoromethyl groups may be the substituents of choice for generating potent ligands of the GlyR.

Fully competitive antagonism was observed with 7TFQA and 7TFQ, which suggests a common binding site for glycine and these compounds. In contrast, the related chloride-substituted analogs 5,7ClQA and 7ClQ displayed both high affinity competitive and low affinity noncompetitive antagonism. The origin of their mixed inhibition profiles is presently unclear; however, because the reduction of the I_{max} value was independent of membrane potential, binding of 5,7ClQA within the ion channel seems unlikely. A mixed competitive and noncompetitive antagonism has also been discussed for the classic GlyR antagonist strychnine, which differs significantly in its molecular structure from 5,7ClQA (30, 31). Thus, a second low affinity binding site exists on the GlyR, which causes allosteric inhibition.

The slopes of the inhibition curves of 7TFQA and 7TFQ, but not of 5,7ClQA and 7ClQ, were strongly dependent on the concentration of coapplied glycine. This seems counterintuitive to the prediction of a parallel shift of concentration-effect curves by competitive inhibitors according to Cheng-Prusoff calculations (32). However, the strong cooperativity of GlyR channel gating implies nonlinear interactions between agonists and antagonists. Using the equation, we could demonstrate that the high Hill coefficient value of glycine (~2.6) results in a hyperbolic plot of IC_{50} values versus agonist concentrations. This finding has important practical implications: neglect of the influence of agonist cooperativity will

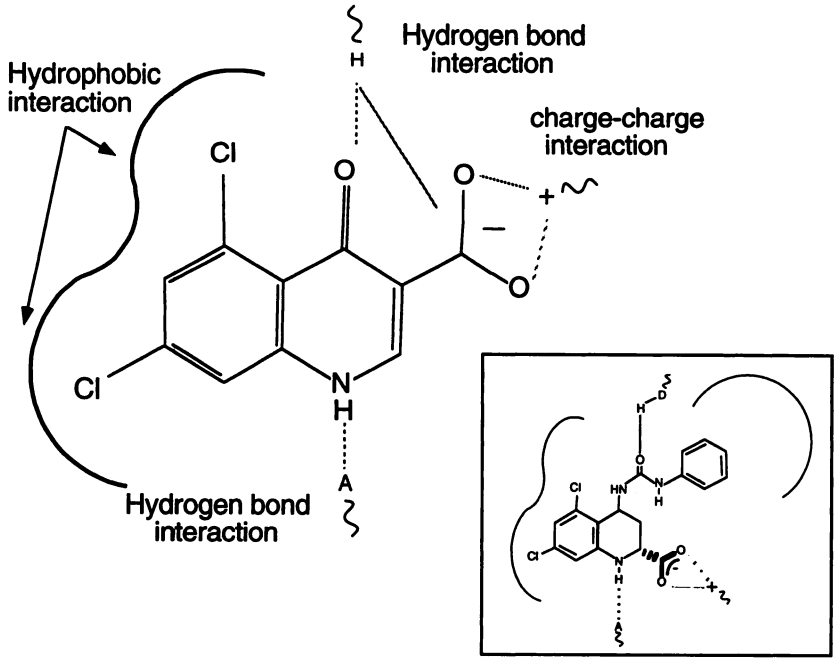

Fig. 6. Model of the pharmacophore of the GlyR. 5,7ClQA is shown with subsites predicted to mediate its binding into the ligand-binding pocket of the GlyR. The halogen-substituted aromatic ring is suggested to interact with a hydrophobic domain of the receptor, whereas hydrogen and charge-charge bonds are proposed to mediate binding of the nitrogen atom and the hydroxyl and carboxylic groups, respectively. *Inset*, analogous model of the binding pocket of the NMDAR (33).

give rise to false K_i estimates and apparent antagonist cooperativity.

Based on the structural similarities between compounds acting at the glycine sites of the GlyR and the NMDAR, we suggest a similar design for the respective binding pockets. A model of the pharmacophore of the GlyR that is analogous to that postulated for the NMDAR (33) is shown in Fig. 6. Because lipophilic ring substitutions increase the potency of quinoline compounds, a hydrophobic receptor domain should exist within the ligand-binding pocket of the GlyR. Additional hydrogen bonds interacting with the nitrogen moiety and the hydroxyl group of the quinoline derivatives are proposed to be localized at similar positions, as suggested for the NMDAR (33). A significant difference, however, must exist in the subsites that interact with the carboxylic group (i.e., position 2 of NMDAR antagonists but position 3 of GlyR active compounds) (Fig. 6). This difference may also contribute to the distinct agonist pharmacology of the glycine-binding sites of these receptors.

In conclusion, we have shown that carboxyl group substitutions at the third ring atom of the quinolinic acids generate selective GlyR antagonists. This finding is consistent with results of our previous study on the inhibition of GlyR activation by piperidine carboxylic acids (26). Our prediction of hydrophobic antagonist/receptor interactions is consistent with mutational analysis of the ligand-binding site of the GlyR (9, 15, 19, 34) and should help in the design of lead compounds that are applicable to the control of motor and sensory functions.

Acknowledgments

We thank H. Guchhalla for synthesizing 5,7ClQA, P. Schloss and V. O'Connor for critical comments on the manuscript, and M. Baier and H. Reitz for secretarial assistance.

References

1. Betz, H. Structure and function of the inhibitory glycine receptor. *Q. Rev. Biophys.* **25**:381–394 (1992).
2. Grenningloh, G., A. Rienitz, B. Schmitt, C. Methfessel, M. Zensen, K. Beyreuther, E. D. Gundelfinger, and H. Betz. The strychnine-binding subunit of the glycine receptor shows homology with nicotinic acetylcholine receptors. *Nature (Lond.)* **328**:215–220 (1987).
3. Grenningloh, G., V. Schmieden, P. Schofield, P. H. Seeburg, T. Siddique, T. K. Mohandas, C.-M. Becker, and H. Betz. *Alpha* subunit variants of the human glycine receptor: primary structures, functional expression and chromosomal localization of the corresponding genes. *EMBO J.* **9**:771–776 (1990).
4. Kuhse, J., V. Schmieden, and H. Betz. Identification and functional expression of a novel ligand binding subunit of the inhibitory glycine receptor. *J. Biol. Chem.* **265**:22317–22320 (1990).
5. Matzenbach, B., Y. Maulet, L. Sefton, B. Courtier, P. Avner, J. L. Guénet, and H. Betz. Structural analysis of mouse glycine receptor α subunit genes. *J. Biol. Chem.* **269**:2607–2612 (1994).
6. Grenningloh, G., I. Pribilla, P. Prior, G. Multhaup, K. Beyreuther, O. Taleb, and H. Betz. Cloning and expression of the 58 kd *beta* subunit of the inhibitory glycine receptor. *Neuron* **4**:963–970 (1990).
7. Langosch, D., L. Thomas, and H. Betz. Conserved quarternary structure of ligand-gated ion channels: the postsynaptic glycine receptor is a pentamer. *Proc. Natl. Acad. Sci. USA* **85**:7394–7398 (1988).
8. Schmieden, V., G. Grenningloh, P. R. Schofield, and H. Betz. Functional expression in *Xenopus* oocytes of the strychnine binding 48 kd subunit of the glycine receptor. *EMBO J.* **8**:695–700 (1989).
9. Schmieden, V., J. Kuhse, and H. Betz. Agonist pharmacology of neonatal and adult glycine receptor *alpha* subunits: identification of amino acid residues involved in taurine activation. *EMBO J.* **11**:2025–2032 (1992).
10. Bormann, J., N. Rundström, H. Betz, and D. Langosch. Residues within transmembrane segment M2 determine chloride conductance of glycine receptor homo- and hetero-oligomers. *EMBO J.* **12**:3729–3737 (1993).
11. Zarbin, M. A., J. K. Wamsley, and M. J. Kuhar. Glycine receptor: light microscopic autoradiographic localization with [^{3}H]strychnine. *J. Neurosci.* **1**:532–547 (1981).
12. Malosio, M.-L., B. Marquèze-Pouey, J. Kuhse, and H. Betz. Wide-spread expression of glycine receptor subunit mRNAs in the adult and developing rat brain. *EMBO J.* **10**:2401–2409 (1991).
13. Becker, C.-M. Convulsants acting at the inhibitory glycine receptor, in *Handbook of Experimental Pharmacology: Selective Neurotoxicity* (H. Herken and F. Hucho, eds.). 539–575 (1992).
14. Kuhse, J., V. Schmieden, and H. Betz. A single amino acid exchange alters the pharmacology of neonatal rat glycine receptor subunit. *Neuron* **5**:867–873 (1990).
15. Schmieden, V., J. Kuhse, and H. Betz. Mutation of glycine receptor subunit creates β-alanine receptor responsive to GABA. *Science (Washington D. C.)* **262**:256–258 (1993).
16. Langosch, D., B. Laube, N. Rundström, V. Schmieden, J. Bormann, and H. Betz. Decreased agonist affinity and chloride conductance of mutant glycine receptors associated with human hereditary hyperekplexia. *EMBO J.* **13**:4223–4228 (1994).
17. Rajendra, S., J. W. Lynch, K. D. Pierce, C. R. French, P. H. Barry, and P. R. Schofield. Startle disease mutations reduce the agonist sensitivity of the human inhibitory glycine receptor. *J. Biol. Chem.* **269**:18739–18742 (1994).

18. Saul, B., V. Schmieden, C. Kling, C. Mülhardt, P. Gass, J. Kuhse, and C. M. Becker. Point mutation of glycine receptor α1 subunit in the spasmodic mouse affects agonist responses. *FEBS Lett.* **350**:71–76 (1994).
19. Vandenberg, R. J., C. A. Handford, and P. R. Schofield. Distinct agonist- and antagonist-binding sites on the glycine receptor. *Neuron* **9**:491–496 (1992).
20. Laube, B., D. Langosch, H. Betz, and V. Schmieden. Hyperekplexia mutations of the glycine receptor unmask the inhibitory subsite for β-amino-acids. *Neuroreport* **6**:897–900 (1995).
21. Rajendra, S., J. W. Lynch, K. D. Pierce, C. R. French, P. H. Barry, and P. R. Schofield. Mutation of an arginine residue in the human glycine receptor transforms β-alanine and taurine from agonists into competitive antagonists. *Neuron* **14**:169–175 (1995).
22. Johnson, J. W., and P. Ascher. Glycine potentiates the NMDA response in cultured mouse brain neurones. *Nature (Lond.)* **325**:529–531 (1987).
23. McBain, C. J., N. W. Kleckner, S. Wyrick, and R. Dingledine. Structural requirements for activation of the glycine coagonist site of *N*-methyl-D-aspartate receptors expressed in *Xenopus* oocytes. *Mol. Pharmacol.* **36**: 556–565 (1989).
24. Curtis, D. R., and J. C. Watkins. The excitation and depression of spinal neurones by structurally related amino acids. *J. Neurochem.* **6**:117–141 (1960).
25. Leeson, P. D., and L. L. Iversen. The glycine site of the NMDA receptor: structure-activity relationships and therapeutic potential. *Med. Chem.* **37**:4053–4067 (1994).
26. Schmieden, V., and H. Betz. Pharmacology of the inhibitory glycine receptor: agonist and antagonist action of amino acids and piperidine carboxylic acid compounds. *Mol. Pharmacol.* **48**:919–927 (1995).
27. Kuryatov, A., B. Laube, H. Betz, and J. Kuhse. Mutational analysis of the glycine binding site of the NMDA receptor: evidence for structural similarity to bacterial amino acid binding proteins. *Neuron* **12**:1291–1300 (1994).
28. Leff, P., and G. Dougall. Further concerns over Cheng-Prusoff analysis. *Trends Pharmacol. Sci.* **14**:110–112 (1993).
29. Pullan, L. M., and R. J. Powel. Comparison of binding at strychnine-sensitive (inhibitory glycine receptor) and strychnine-insensitive (N-methyl-D-aspartate receptor) glycine binding sites. *Neurosci. Lett.* **148**: 199–201 (1992).
30. Marvizon, J. C., J. Vazquez, M. Garcia-Calvo, F. Mayor, Jr., A. Ruiz-Gomez, F. Valdivieso, and J. Benavides. The glycine receptor: pharmacological studies and mathematical modeling of the allosteric interaction between the glycine- and strychnine-binding sites. *Mol. Pharmacol.* **30**: 590–597 (1986).
31. Suzuki, S., M. Tachibana, and A. Kaneko. Effects of glycine and GABA on isolated bipolar cells of the mouse retina. *J. Physiol. (Lond.)* **421**:645–662 (1990).
32. Cheng, Y.-C., and W. H. Prusoff. Relationship between the inhibition constant (Ki) and the concentration of inhibitor which causes 50 per cent inhibition (IC50) of an enzymatic reaction. *Biochem. Pharmacol.* **84**:3099–3108 (1973).
33. Kemp, J. A., and P. D. Leeson. The glycine site of the NMDA receptor: five years on. *Trends Pharmacol. Sci.* **14**:21–25 (1993).
34. Kuhse, J., Betz, H., and J. Kirsch. The inhibitory glycine receptor: architecture, synaptic localization and molecular pathology of a postsynaptic ion-channel complex. *Curr. Opin. Neurobiol.* **5**:318–323 (1995).

Send reprint requests to: Dr. Volker Schmieden, Max-Planck-Institute for Brain Research, Neurochemistry, Deutschordenstrasse 46, D-60528 Frankfurt, Germany